nature biotechnology

Photoactivatable CRISPR-Cas9 for optogenetic genome editing

Yuta Nihongaki, Fuun Kawano, Takahiro Nakajima & Moritoshi Sato

We describe an engineered photoactivatable Cas9 (paCas9) that enables optogenetic control of CRISPR-Cas9 genome editing in human cells. paCas9 consists of split Cas9 fragments and photoinducible dimerization domains named Magnets. In response to blue light irradiation, paCas9 expressed in human embryonic kidney 293T cells induces targeted genome sequence modifications through both nonhomologous end joining and homology-directed repair pathways. Genome editing activity can be switched off simply by extinguishing the light. We also demonstrate activation of paCas9 in spatial patterns determined by the sites of irradiation. Optogenetic control of targeted genome editing should facilitate improved understanding of complex gene networks and could prove useful in biomedical applications.

© 2015 Nature America, Inc. All rights reserved.

The type II bacterial clustered, regularly interspaced, short palindromic repeats (CRISPR) and the CRISPR-associated protein 9 (Cas9), known as CRISPR-Cas9, mediates targeted genome modifications that enable dissection of gene and regulatory functions[1–3]. The *Streptococcus pyogenes* Cas9 nuclease (hereafter referred to as Cas9) can bind to and cleave a target DNA sequence that is complementary to the first 20 nucleotides of a single-guide RNA (sgRNA) and is adjacent to a protospacer-adjacent motif (PAM) of the form NGG. Cas9-induced DNA double-strand breaks are repaired by nonhomologous end joining (NHEJ) or homology-directed repair (HDR) in mammalian cells, thereby enabling targeted genome editing.

Methods have been developed to chemically control the nuclease activity of Cas9, such as doxycycline-regulated Cas9 expression[4,5], rapamycin-inducible split-Cas9 (ref. 6) and transient delivery of purified Cas9:sgRNA complex[7–9]. These chemical methods have been used for generating conditional gene knockouts and reducing levels of off-target genome modification. However, some chemicals have adverse effects. For example, rapamycin can induce undesirable biological effects by perturbing the endogenous mammalian target of rapamycin (mTOR) pathway[10]. Also, because chemicals diffuse freely and are difficult to rapidly remove, such methods cannot be applied to achieve spatiotemporal genome editing.

We set out to design a method of controlling Cas9 nuclease activity that is noninvasive and incorporates spatial, temporal and reversible control. Light has high spatiotemporal resolution and is noninvasive[11,12] but methods to optically control Cas9 nuclease activity have so far been elusive.

To produce an optically controlled Cas9 we fused two split Cas9 fragments with photoinducible dimerization domains to generate paCas9 (**Fig. 1a**). In initial experiments to determine the best suited split site of Cas9 for high efficiency inducible control, we generated various Cas9 fragments fused with the rapamycin-inducible dimerization system, FKBP-FRB[13] (**Supplementary Fig. 1**). We selected 18 candidate split sites based on an analysis of the crystal structure of Cas9 in complex with sgRNA[14,15]. All candidate split site positions were loop regions exposed to solvent. We assessed the rapamycin-induced nuclease activity of each split-Cas9 pair using a luciferase-reporter plasmid HDR assay (**Fig. 1b**). In this assay, the cytomegalovirus (CMV) promoter-driven luciferase reporter with an in-frame stop codon (StopFluc-1) is cleaved by split-Cas9, and then recovers full-length luciferase expression through homologous recombination with promoter-less luciferase donor vector. Eight combinations of N- and C-terminal Cas9 fragments showed significant rapamycin-induced reporter upregulation in HEK293T cells (**Supplementary Fig. 2**). In subsequent experiments, we used the N-terminal fragment of Cas9 (residues 2–713, named N713) and C-terminal fragment of Cas9 (residues 714–1,368, named C714), which was one of the most effective rapamycin-inducible split-Cas9 pairs.

Next, we fused photoinducible dimerization domains with N713 and C714 (**Fig. 1c**). First, we tested the CRY2-CIB1 photoinducible dimerization system, which is based on blue light–dependent protein interactions between *Arabidopsis thaliana* cryptochrome 2 (CRY2) and its binding partner CIB1 (ref. 16). This system has been widely used for optogenetic control of protein-protein interactions in mammalian cells. We generated N713 and C714 fused to the photolyase homology region of CRY2 (CRY2PHR) and CIB1 and tested induction potency using a luciferase plasmid HDR assay. However, N713 and C714 fused to the CRY2PHR and CIB1 system did not show light-induced Cas9 activity. There are several possible explanations for this failure. First, steric hindrance could be caused by CRY2PHR (498 amino acids) and CIB1 (335 amino acids), impeding reassembly of split-Cas9. Second, oligomerization of CRY2PHR might reduce or preclude interactions between the N-terminal and C-terminal fragments of Cas9 (ref. 17). Keeping these potential problems in mind we next focused on a recently developed photoinducible dimerization system named Magnets[18]. The Magnet system consists of paired photoswitchable proteins, named positive Magnet (pMag) and negative Magnet (nMag). Upon blue light irradiation, pMag and nMag heterodimerize. Unlike CRY2-CIB1, pMag and nMag (150 amino

Graduate School of Arts and Sciences, The University of Tokyo, Komaba, Meguro-ku, Tokyo, Japan. Correspondence should be addressed to M.S. (cmsato@mail.ecc.u-tokyo.ac.jp).

Received 21 February; accepted 5 May; published online 15 June 2015; doi:10.1038/nbt.3245

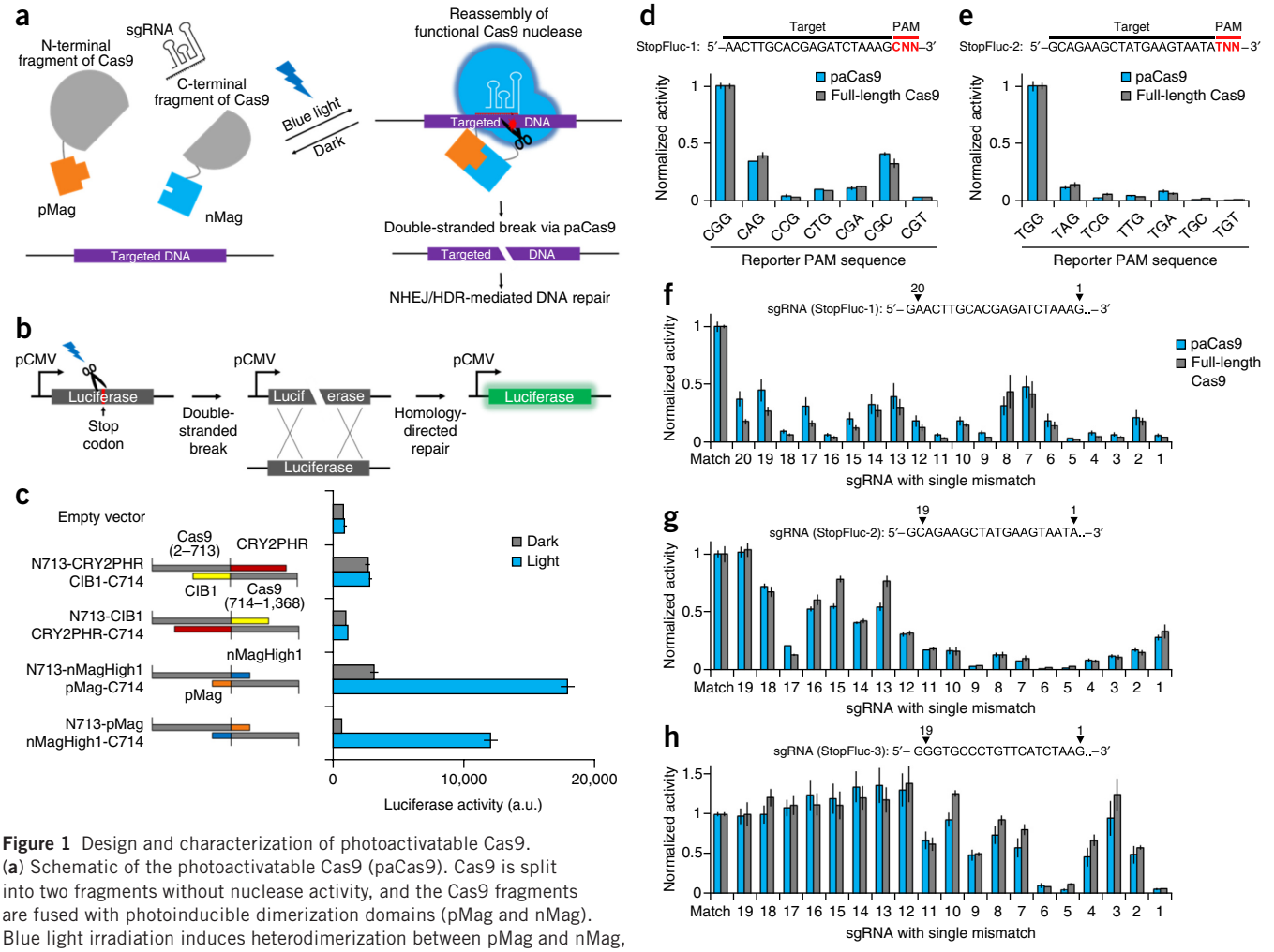


Figure 1 Design and characterization of photoactivatable Cas9. (**a**) Schematic of the photoactivatable Cas9 (paCas9). Cas9 is split into two fragments without nuclease activity, and the Cas9 fragments are fused with photoinducible dimerization domains (pMag and nMag). Blue light irradiation induces heterodimerization between pMag and nMag, which enables split Cas9 fragments to reassociate, thereby reconstituting RNA-guided nuclease activity. Gray, inactive; blue, active. (**b**) Luciferase reporter plasmid HDR assay. When Cas9 cleaves the CMV-driven luciferase reporter with an in-frame stop codon (StopFluc-1), the luciferase reporter is repaired by homologous recombination with promoter-less luciferase donor vector and recovers bioluminescence activity. (**c**) Light-induced reporter activity in HEK293T cells using N713 and C714 fragments of Cas9 fused with photoinducible dimerization domains. (**d**,**e**) Activities of paCas9-1 and full-length Cas9 targeting StopFluc-1 (**d**) and StopFluc-2 (**e**), harboring indicated mutations in the PAM. Values are normalized to a positive control, which is a luciferase reporter with canonical PAM (NGG). (**f**–**h**) Activities of Cas9 and paCas9 targeting StopFluc-1 (**f**), StopFluc-2 (**g**) and StopFluc-3 (**h**) with a set of sgRNAs harboring single-nucleotide Watson-Crick transversion mutations. sgRNAs mutated in 5′-end G to C were not tested because 5′-end G is necessary for efficient expression from the U6 promoter. The positions of point mutations in each sgRNA are indicated at the top of each panel. Values are normalized to positive control with perfectly matched sgRNAs. In (**c**–**h**), data are shown as the mean ± s.e.m. ($n = 6$ from two individual experiments with biological triplicates that is, separately seeded cells).

acids each) are of a similar size to FKBP (107 amino acids) and FRB (93 amino acids). The dynamic range and dissociation kinetics of the Magnet system can be tuned by mutating pMag and/or nMag. We used pMag and nMagHigh1 (nMag with M135I and M165I mutations)[18]. To test whether Magnets could provide effective light-triggered reassembly of a split-Cas9, we tested two pairs of fusion proteins; N713-nMagHigh1 and pMag-C714 and N713-pMag and nMagHigh1-C714. We found that both paired fusion proteins showed substantial light-induced Cas9 activity, and N713-pMag and nMagHigh1-C714 yielded the highest fold-induction (16.4-fold) and lowest background activity (**Fig. 1c**). We used N713-pMag and nMagHigh1-C714 and named this construct paCas9-1 (**Supplementary Fig. 3**).

To investigate whether paCas9-1 recognizes PAM in the same way as full-length Cas9, we generated a set of luciferase reporters, into which we inserted stop codons, and which harbored a point mutation in NGG PAM (**Fig. 1d**,**e**). We tested two different luciferase reporters containing an internal stop codon in different sites (StopFluc-1 and StopFluc-2) and confirmed that the Cas9-induced activities of the luciferase reporters that had noncanonical PAM were lower than that of luciferase reporters having the canonical PAM of the form NGG. We found no significant difference in the normalized luciferase activities of paCas9-1 and full-length Cas9. We also evaluated the DNA targeting specificity of paCas9-1 using a luciferase plasmid HDR assay (**Fig. 1f**). We produced a series of sgRNAs for StopFluc-1 harboring single-nucleotide Watson-Crick transversion mutations (**Supplementary Table 1**). We found no significant difference in the DNA targeting specificities of paCas9-1 and full-length Cas9. To further investigate DNA targeting specificity of paCas9-1, we performed the specificity assay using two different reporters containing an internal stop codon in different sites (StopFluc-2 and StopFluc-3) and confirmed that the DNA targeting specificity of paCas9-1 is comparable with that of full-length Cas9 (**Fig. 1g**,**h**). Consistent with previous

© 2015 Nature America, Inc. All rights reserved.

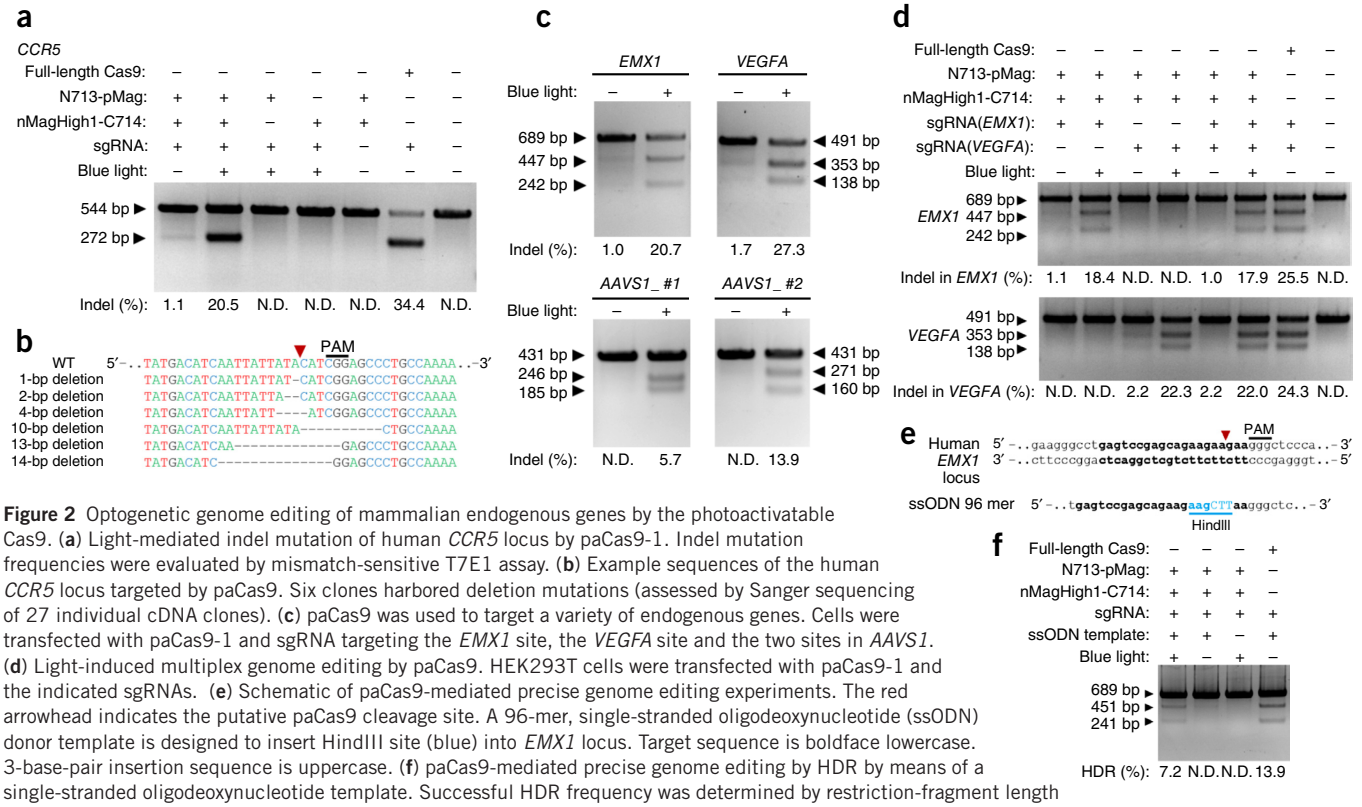


Figure 2 Optogenetic genome editing of mammalian endogenous genes by the photoactivatable Cas9. (**a**) Light-mediated indel mutation of human *CCR5* locus by paCas9-1. Indel mutation frequencies were evaluated by mismatch-sensitive T7E1 assay. (**b**) Example sequences of the human *CCR5* locus targeted by paCas9. Six clones harbored deletion mutations (assessed by Sanger sequencing of 27 individual cDNA clones). (**c**) paCas9 was used to target a variety of endogenous genes. Cells were transfected with paCas9-1 and sgRNA targeting the *EMX1* site, the *VEGFA* site and the two sites in *AAVS1*. (**d**) Light-induced multiplex genome editing by paCas9. HEK293T cells were transfected with paCas9-1 and the indicated sgRNAs. (**e**) Schematic of paCas9-mediated precise genome editing experiments. The red arrowhead indicates the putative paCas9 cleavage site. A 96-mer, single-stranded oligodeoxynucleotide (ssODN) donor template is designed to insert HindIII site (blue) into *EMX1* locus. Target sequence is boldface lowercase. 3-base-pair insertion sequence is uppercase. (**f**) paCas9-mediated precise genome editing by HDR by means of a single-stranded oligodeoxynucleotide template. Successful HDR frequency was determined by restriction-fragment length polymorphism (RFLP) analysis, and calculated as the ratio of HindIII digested product to substrate. NHEJ and HDR rates presented are means N.D., not determined. (In **a**, $n = 3$ from independent experiments. In **c**,**d** and **f**, $n = 2$ from two independent experiments.) In **a**,**c**,**d**,**f**, 20 h after transfection, samples were illuminated by 1.2 W/m^2 blue light or kept in the dark for 24 h (**a**,**c**,**d**) or 48 h (**f**) before genome extraction. Full-length gels are presented in **Supplementary Figure 8**.

studies, sensitivity patterns to single sgRNA-DNA mismatch differed among target sequences[19–21]. From these experiments, we conclude that the PAM requirement and target specificities of paCas9-1 are indistinguishable from those of full-length Cas9.

To show that paCas9-1 could cleave a targeted endogenous genomic locus in mammalian cells and induce indel mutation by nonhomologous end joining (NHEJ) in a light-dependent fashion, we transfected HEK293T cells with paCas9-1 and an sgRNA targeting the human *CCR5* locus (**Fig. 2a**). We quantitatively evaluated the ability of paCas9-1 to induce indel mutations in response to light using the mismatch-sensitive T7 endonuclease I (T7E1), which cleaves heteroduplexed DNA strands formed by hybridization between mutant and wild-type DNA. In the dark, cells transfected with paCas9-1 targeting *CCR5* showed only 1.1% indel rates. However, upon blue light irradiation, cells transfected with paCas9-1 targeting *CCR5* exhibited significantly ($P = 0.012$) higher indel rates (20.5%) in the human *CCR5* locus. The frequency of indel mutations induced by paCas9-1 is ~60% of that achievable with full-length Cas9 (paCas9-1: 20.5%, full-length Cas9: 34.4%) (**Fig. 2a**). Using Sanger sequencing, we verified that paCas9-1–mediated indel mutations occurred in the targeted region of the human *CCR5* locus (**Fig. 2b**). To explore the generalizability of optogenetic RNA-guided genome editing with paCas9-1, we used sgRNAs for four additional sites in three human genes (*EMX1*, *VEGFA* and *AAVS1*). With each of these sgRNAs, we observed light-induced indel mutations were observed (**Fig. 2c**). We also carried out a time-course analysis of indel mutations in the *EMX1* locus induced by paCas9-1 (**Supplementary Fig. 4**). We observed that the frequency of indel mutations increased as the blue light irradiation time increased. To test whether paCas9-1 could induce indel mutations in different cell lines, we transfected HeLa cells with paCas9-1 and an sgRNA targeting human *EMX1* (**Supplementary Fig. 5**). Light-induced indel mutations in the *EMX1* locus were also observed in HeLa cells. We also tested whether paCas9-1 could induce indel mutations at multiple target sites (**Fig. 2d**). Using two sgRNAs targeting *EMX1* and *VEGFA* simultaneously, paCas9-1 induced indel mutations in both human *EMX1* and *VEGFA* loci in response to light. These results show that paCas9-1 can be deployed for optogenetic multiplexed control of NHEJ-mediated indel mutations in mammalian cells.

Next, we investigated whether paCas9-1 could be used for genome editing by means of HDR (**Fig. 2e**,**f**). We used single-stranded oligodeoxynucleotides (ssODN) as a donor template. We transfected HEK293T cells with paCas9-1 targeting *EMX1* and ssODN containing a HindIII site and analyzed the frequency of HDR in the EMX1 locus using a restriction fragment length polymorphism (RFLP) assay. We found that paCas9-1 induces HindIII site integration in the human *EMX1* locus at a frequency of 7.2%. This shows that paCas9-1 can induce both random indel mutations and designed genome sequence modification through HDR in response to light.

The off-target activity of Cas9 has been reduced using a paired nicking strategy based on the Cas9 D10A variant, which nicks targeted DNA instead of cutting double strands[22]. To explore whether paCas9-1 could be converted into a photoactivatable nickase, we produced paCas9-1 containing the D10A mutation (paCas9 nickase) (**Supplementary Fig. 6**). Using the paCas9 nickase with an sgRNA targeting *EMX1* did not induce indel mutations in the human *EMX1* locus. However, using a pair of sgRNAs targeting opposite strands of the *EMX1* site, our paCas9 nickase induced indel mutations in

© 2015 Nature America, Inc. All rights reserved.

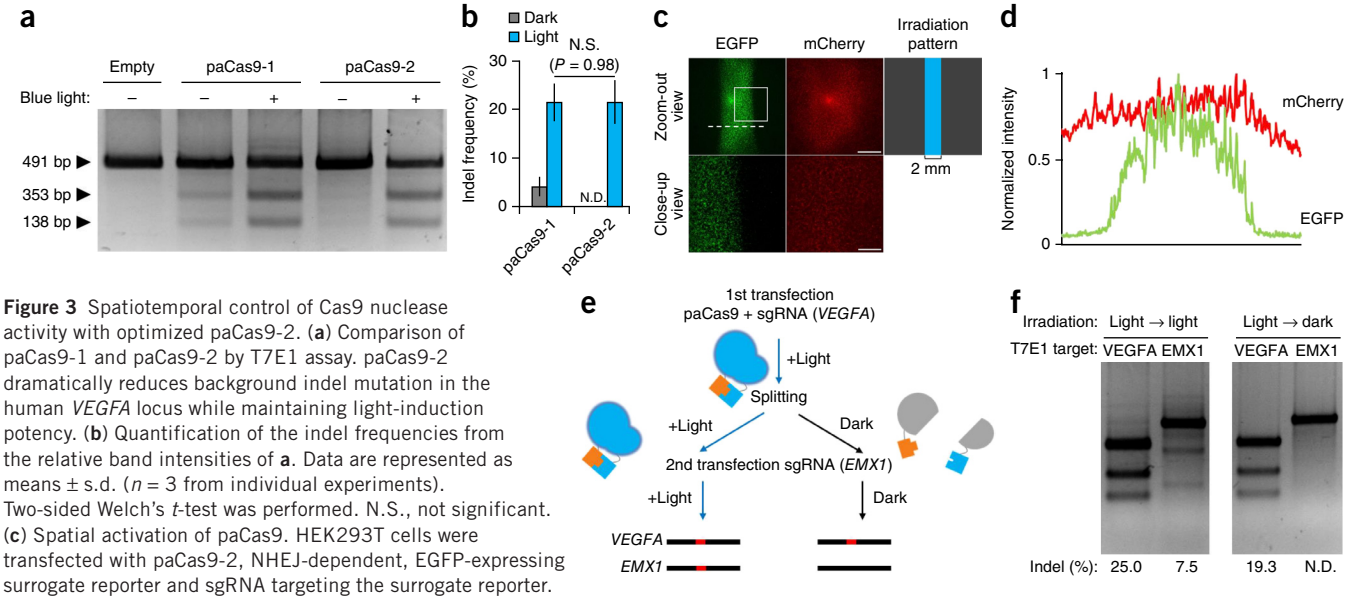


Figure 3 Spatiotemporal control of Cas9 nuclease activity with optimized paCas9-2. (**a**) Comparison of paCas9-1 and paCas9-2 by T7E1 assay. paCas9-2 dramatically reduces background indel mutation in the human *VEGFA* locus while maintaining light-induction potency. (**b**) Quantification of the indel frequencies from the relative band intensities of **a**. Data are represented as means ± s.d. ($n = 3$ from individual experiments). Two-sided Welch's *t*-test was performed. N.S., not significant. (**c**) Spatial activation of paCas9. HEK293T cells were transfected with paCas9-2, NHEJ-dependent, EGFP-expressing surrogate reporter and sgRNA targeting the surrogate reporter. 20 h after transfection, samples were irradiated by slit-patterned blue light using a photomask for 24 h. The width of the slit is 2 mm. Close-up view within white square region is also shown. Scale bar, 3 mm (zoom-out view) and 1 mm (close-up view), respectively. (**d**) Line scan intensity profile of EGFP (green) and mCherry (red) in **c**. (**e**) Experimental scheme to test whether paCas9 activation is reversible. First, HEK293T cells were transfected with paCas9-2 and sgRNA targeting *VEGFA*. After 20 h, cells were illuminated with blue light for 6 h, then split and incubated in the light or the dark. After 6 h incubation, the cells were transfected with an sgRNA targeting *EMX1*, and incubated again in the light or the dark. 30 h later, genomic DNA was extracted. If paCas9 activation is reversible, the cells shifted to the dark state before the second transfection of sgRNA targeting *EMX1* should show the indel mutation in only the *VEGFA* locus. (**f**) A representative gel of the T7E1 assay in **e**. The indel frequencies of the *EMX1* and *VEGFA* locus are shown at the bottom of the gel. ($n = 4$ from two independent experiments with biological duplicates). Full-length gels are presented in **Supplementary Figure 8**.

response to light. This indicates that the double-nicking strategy can be applied to paCas9 to reduce off-target genome modifications.

Although paCas9-1 can induce efficient NHEJ-mediated indel mutation, paCas9-1 had background activity (about 1–3%) in the dark (**Fig. 2a**,**c**). To reduce the background activity of paCas9-1, we replaced nMagHigh1-C714 with nMag-C714 because the combination of pMag and nMag shows lower background activity than that of pMag and nMagHigh1 (ref. 18). We transfected HEK293T cells with N713-pMag, nMag-C714 (named paCas9-2) and an sgRNA targeting *VEGFA* locus, and measured induced indel mutations in the light and the dark (**Fig. 3a**). The frequency of indel mutations in the dark induced by paCas9-2 was reduced to an undetectable level, as monitored using the T7E1 assay. Note that the light-induced indel frequency with paCas9-2 is comparable to that obtained using paCas9-1 (**Fig. 3b**). Therefore, we used paCas9-2 in all subsequent experiments.

Next, we tested whether paCas9 can enable light-induced spatial activation of genome editing (**Fig. 3c**,**d** and **Supplementary Fig. 7**). To visualize Cas9-induced NHEJ-mediated indel mutations in living cells, we used a surrogate EGFP reporter system that expresses EGFP fluorescence when a double-strand break is introduced into the target sequence by Cas9 (refs. 23,24). HEK293T cells transfected with paCas9-2, surrogate EGFP reporter and sgRNA targeting reporter were irradiated with slit-patterned blue light. After 24 h, a slit pattern of EGFP-expression was observed, showing that paCas9-2 can spatially control gene editing in response to light.

We also investigated whether paCas9 activation is reversible (**Fig. 3e**,**f**). We first transfected HEK293T cells with paCas9-2 and an sgRNA targeting *VEGFA*, and incubated these samples with blue-light irradiation to induce paCas9-2 activation. After 6 h, we split the cells and incubated half the cells in the dark and half the cells in light. After 6 h incubation in the dark or light, we performed a second transfection of an sgRNA targeting *EMX1*. The cells that had been incubated in the dark just before the second transfection were incubated again in the dark state, whereas the cells incubated in light before the second transfection were incubated again in light. After 30 h incubation, the genomic DNA was isolated and analyzed by T7E1 assay. Cells irradiated with blue light after the first transfection of paCas9-2 and with sgRNA targeting *VEGFA* showed indel mutations in the *VEGFA* locus, indicating that paCas9-2 was activated by the blue light. After the second transfection with an sgRNA targeting *EMX1*, cells irradiated continuously with blue light showed indel mutations in the *EMX1* locus; however, cells shifted to the dark did not have indel mutations in *EMX1* locus. This result indicates that paCas9-2 can be reversibly activated by blue light.

Several reports have shown that RNA-guided targeting of catalytically inactive Cas9 (dCas9) to a specific gene can sterically block RNA polymerase and transcript elongation, enabling RNA-guided gene silencing, which has been named CRISPR interference (CRISPRi)[25]. To further demonstrate the utility of paCas9, we tested photoactivatable and reversible control of CRISPRi. We named this method photoactivatable CRISPRi (paCRISPRi). To do this, we generated paCas9-2 containing D10A and H840A mutations (padCas9) (**Fig. 4a**). We also designed three sgRNAs targeting different regions of the CMV promoter-driven luciferase reporter containing PEST (proline-glutamate-serine-threonine rich) and mRNA destabilizing sequences[26]. padCas9 with each sgRNA targeting the luciferase reporter showed light-induced repression of luciferase reporter activity (**Fig. 4b**), demonstrating that our paCas9 platform also provides optogenetic control of RNA-guided transcription. We also found that the repression efficiency of padCas9 is slightly lower than that of full-length dCas9 (**Fig. 4c**). This is consistent with the fact that the frequency of indel mutation induced by paCas9 is ~60% of that achievable with full-length Cas9 (**Fig. 2a**). Efficiency might be improved by further engineering of padCas9 to, for instance,

© 2015 Nature America, Inc. All rights reserved.

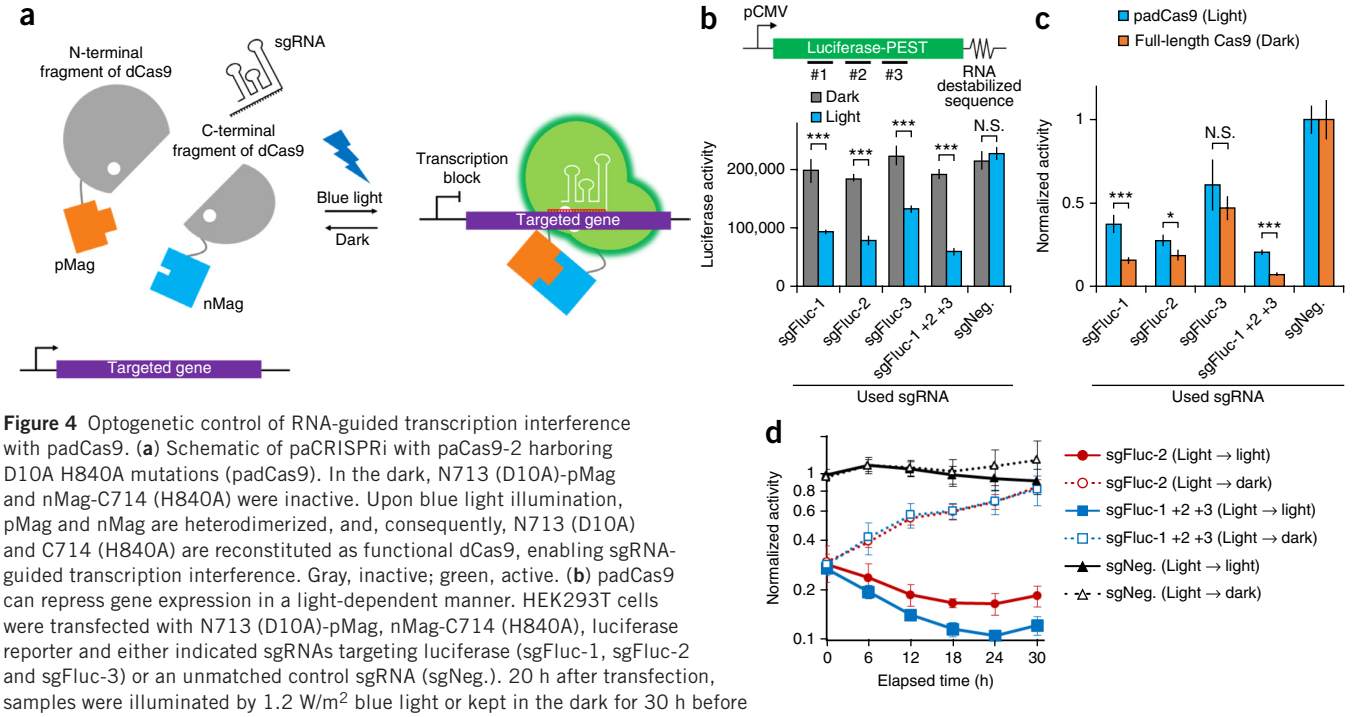


Figure 4 Optogenetic control of RNA-guided transcription interference with padCas9. (**a**) Schematic of paCRISPRi with paCas9-2 harboring D10A H840A mutations (padCas9). In the dark, N713 (D10A)-pMag and nMag-C714 (H840A) were inactive. Upon blue light illumination, pMag and nMag are heterodimerized, and, consequently, N713 (D10A) and C714 (H840A) are reconstituted as functional dCas9, enabling sgRNA-guided transcription interference. Gray, inactive; green, active. (**b**) padCas9 can repress gene expression in a light-dependent manner. HEK293T cells were transfected with N713 (D10A)-pMag, nMag-C714 (H840A), luciferase reporter and either indicated sgRNAs targeting luciferase (sgFluc-1, sgFluc-2 and sgFluc-3) or an unmatched control sgRNA (sgNeg.). 20 h after transfection, samples were illuminated by 1.2 W/m^2 blue light or kept in the dark for 30 h before measuring luciferase bioluminescence. In this experiment, a luciferase reporter containing PEST and mRNA destabilized sequence was used. Data are represented as the mean ± s.e.m. (n = 6 from two individual experiments with biological triplicates). Two-sided Welch's t-test was carried out. N.S., not significant; ***P < 0.005 versus the sample in the dark. (**c**) Comparison of the repression efficiency of padCas9 and full-length dCas9. Values are normalized to negative control with an unmatched control sgRNA (sgNeg.). Data are represented as the mean ± s.e.m. (n = 6 from two individual experiments with biological triplicates). Two-sided Welch's t-test was performed. N.S., not significant; *P < 0.05; ***P < 0.005 versus the full-length dCas9 in the dark. (**d**) Time-course of restored luciferase reporter activity after blue light irradiation. HEK293T cells were transfected with N713 (D10A)-pMag, nMag-C714 (H840A), luciferase reporter and the indicated sgRNAs. Immediately after transfection, samples were illuminated by 1.2 W/m^2 blue light for 30 h before measuring bioluminescence at time 0. After time 0 measurement, samples were illuminated by 1.2 W/m^2 blue light (solid lines) or kept in the dark (dotted lines), and bioluminescence was measured every 6 h. Data are shown as mean ± s.e.m. (n = 6 from two individual experiments with biological triplicates) normalized to negative control cells (under continuous light irradiation) at time 0.

optimize the protein stability, nuclear localization and dynamic range of photoinducible domains. We also tested whether padCas9-mediated gene repression could be switched off by halting light irradiation (**Fig. 4d**). We found that the reporter activity recovered gradually after we turned off the blue light, showing that CRISPRi with padCas9 is reversible. Collectively, our results show that paCas9 can offer spatiotemporal control of RNA-guided genome editing and transcription regulation in a reversible manner.

A rapamycin-inducible Cas9 designed with a split-Cas9 architecture that is similar to ours has recently been reported[6]. However, rapamycin-inducible Cas9 does not offer spatial and reversible activation because rapamycin diffuses freely and is hard to remove[27]. Furthermore, rapamycin can perturb endogenous mTOR signaling pathways[10].

The spatiotemporal and reversible properties of paCas9 are well suited for the dissection of causal gene function in diverse biological processes and for medical applications, such as *in vivo* and *ex vivo* gene therapies. Also, paCas9 has the potential to reduce off-target indel frequencies in Cas9-based genome editing. There are several studies showing that transient introduction of a Cas9:sgRNA complex prepared *in vitro* can improve the specificity of genome editing[7–9]. Because paCas9 can be switched off by stopping light irradiation, optically controlling the duration of paCas9 activation would contribute to reducing off-target gene modification.

This paCas9 platform has the potential to further facilitate CRISPR-Cas9 applications. For example, Cas9 applications *in vivo* have been limited owing to the packaging size limitation of viral vectors. Because the cDNA of our paCas9 components is shorter than that of full-length Cas9, it will be possible to separately package each paCas9 fragment into viral vectors having size limitation, expanding the opportunities of *in vivo* genome editing. Another potential application of paCas9 is intersectional control of Cas9 activity, enabling conditional genome editing with high precision. Recently, a conditional gene knockout strategy has been developed, by combining Cas9 and tissue-specific promoter[28]. By expressing each paCas9 component from two different tissue-specific promoters, Cas9 activity could be controlled by two promoter activities and light, enabling gene modification with ultrahigh precision.

We and other groups have recently reported dCas9-based photoactivatable transcription systems[29,30]. These dCas9-based optogenetic systems can activate targeted endogenous gene expression. Unlike these systems, the paCas9 described in this manuscript enables light-inducible targeted genome editing by NHEJ and HDR pathways. In addition, we show that paCRISPRi enables optogenetic control of targeted gene silencing.

METHODS

Methods and any associated references are available in the online version of the paper.

Note: Any Supplementary Information and Source Data files are available in the online version of the paper.

© 2015 Nature America, Inc. All rights reserved.

ACKNOWLEDGMENTS
We would like to thank J. Galipon for technical assistance. This work was supported by Platform for Dynamic Approaches to Living System from the Ministry of Education, Culture, Sports, Science and Technology, Japan (MEXT) and by grants from Japan Society for the Promotion of Science (JSPS).

AUTHOR CONTRIBUTIONS
Y.N. and M.S. conceived the project. Y.N., F.K., T.N. and M.S. designed the experiments. Y.N. performed experiments and analyzed data. Y.N. and M.S. wrote the manuscript.

COMPETING FINANCIAL INTERESTS
The authors declare no competing financial interests.

Reprints and permissions information is available online at http://www.nature.com/reprints/index.html.

1. Cong, L. *et al.* Multiplex genome engineering using CRISPR/Cas systems. *Science* **339**, 819–823 (2013).
2. Mali, P. *et al.* RNA-guided human genome engineering via Cas9. *Science* **339**, 823–826 (2013).
3. Jinek, M. *et al.* RNA-programmed genome editing in human cells. *Elife* **2**, e00471 (2013).
4. Dow, L.E. *et al.* Inducible in vivo genome editing with CRISPR-Cas9. *Nat. Biotechnol.* **33**, 390–394 (2015).
5. González, F. *et al.* An iCRISPR platform for rapid, multiplexable, and inducible genome editing in human pluripotent stem cells. *Cell Stem Cell* **15**, 215–226 (2014).
6. Zetsche, B., Volz, S.E. & Zhang, F. A split-Cas9 architecture for inducible genome editing and transcription modulation. *Nat. Biotechnol.* **33**, 139–142 (2015).
7. Kim, S., Kim, D., Cho, S.W., Kim, J. & Kim, J.-S. Highly efficient RNA-guided genome editing in human cells via delivery of purified Cas9 ribonucleoproteins. *Genome Res.* **24**, 1012–1019 (2014).
8. Zuris, J.A. *et al.* Cationic lipid-mediated delivery of proteins enables efficient protein-based genome editing *in vitro* and *in vivo*. *Nat. Biotechnol.* **33**, 73–80 (2015).
9. Ramakrishna, S. *et al.* Gene disruption by cell-penetrating peptide-mediated delivery of Cas9 protein and guide RNA. *Genome Res.* **24**, 1020–1027 (2014).
10. Laplante, M. & Sabatini, D.M. mTOR signaling in growth control and disease. *Cell* **149**, 274–293 (2012).
11. Brieke, C., Rohrbach, F., Gottschalk, A., Mayer, G. & Heckel, A. Light-controlled tools. *Angew. Chem. Int. Edn Engl.* **51**, 8446–8476 (2012).
12. Lee, H., Larson, D. & Lawrence, D. Illuminating the chemistry of life: design, synthesis, and applications of "caged" and related photoresponsive compounds. *ACS Chem. Biol.* **4**, 409–427 (2009).
13. DeRose, R., Miyamoto, T. & Inoue, T. Manipulating signaling at will: chemically-inducible dimerization (CID) techniques resolve problems in cell biology. *Pflugers Arch.* **465**, 409–417 (2013).
14. Nishimasu, H. *et al.* Crystal structure of Cas9 in complex with guide RNA and target DNA. *Cell* **156**, 935–949 (2014).
15. Anders, C., Niewoehner, O., Duerst, A. & Jinek, M. Structural basis of PAM-dependent target DNA recognition by the Cas9 endonuclease. *Nature* **513**, 569–573 (2014).
16. Kennedy, M.J. *et al.* Rapid blue-light–mediated induction of protein interactions in living cells. *Nat. Methods* **7**, 973–975 (2010).
17. Bugaj, L.J., Choksi, A.T., Mesuda, C.K., Kane, R.S. & Schaffer, D.V. Optogenetic protein clustering and signaling activation in mammalian cells. *Nat. Methods* **10**, 249–252 (2013).
18. Kawano, F., Suzuki, H., Furuya, A. & Sato, M. Engineered pairs of distinct photoswitches for optogenetic control of cellular proteins. *Nat. Commun.* **6**, 6256 (2015).
19. Hsu, P.D. *et al.* DNA targeting specificity of RNA-guided Cas9 nucleases. *Nat. Biotechnol.* **31**, 827–832 (2013).
20. Mali, P. *et al.* CAS9 transcriptional activators for target specificity screening and paired nickases for cooperative genome engineering. *Nat. Biotechnol.* **31**, 833–838 (2013).
21. Fu, Y. *et al.* High-frequency off-target mutagenesis induced by CRISPR-Cas nucleases in human cells. *Nat. Biotechnol.* **31**, 822–826 (2013).
22. Ran, F.A. *et al.* Double nicking by RNA-guided CRISPR Cas9 for enhanced genome editing specificity. *Cell* **154**, 1380–1389 (2013).
23. Kim, H. *et al.* Surrogate reporters for enrichment of cells with nuclease-induced mutations. *Nat. Methods* **8**, 941–943 (2011).
24. Ramakrishna, S. *et al.* Surrogate reporter-based enrichment of cells containing RNA-guided Cas9 nuclease-induced mutations. *Nat. Commun.* **5**, 3378 (2014).
25. Qi, L.S. *et al.* Repurposing CRISPR as an RNA-guided platform for sequence-specific control of gene expression. *Cell* **152**, 1173–1183 (2013).
26. Voon, D.C. *et al.* Use of mRNA- and protein-destabilizing elements to develop a highly responsive reporter system. *Nucleic Acids Res.* **33**, e27 (2005).
27. Lin, Y. *et al.* Rapidly reversible manipulation of molecular activity with dual chemical dimerizers. *Angew. Chem. Int. Edn Engl.* **52**, 6450–6454 (2013).
28. Shen, Z. *et al.* Conditional knockouts generated by engineered CRISPR-Cas9 endonuclease reveal the roles of coronin in *C. elegans* neural development. *Dev. Cell* **30**, 625–636 (2014).
29. Nihongaki, Y., Yamamoto, S., Kawano, F., Suzuki, H. & Sato, M. CRISPR-Cas9-based photoactivatable transcription system. *Chem. Biol.* **22**, 169–174 (2015).
30. Polstein, L.R. & Gersbach, C.A. A light-inducible CRISPR-Cas9 system for control of endogenous gene activation. *Nat. Chem. Biol.* **11**, 198–200 (2015).

© 2015 Nature America, Inc. All rights reserved.

ONLINE METHODS

Inducible Cas9 constructions. cDNAs encoding the N- and C-terminals fragments of codon-optimized *S. pyogenes* Cas9 fused with a nuclear localization signal from SV40 were amplified from Addgene plasmid 42230. cDNAs encoding FKBP and FRB were amplified from a human cDNA library. cDNA encoding CRY2PHR was amplified from Addgene plasmid 26871. The plasmid containing CIB1 was obtained from RIKEN BioResource Center (resource number: pda10875). cDNA encoding pMag, nMagHigh1 and nMag was prepared as previously described[18]. These inducible dimerization domains were amplified by standard PCR using primers that add glycine-serine linker sequences at the 5′ and 3′ ends. The inducible Cas9 constructs based on the N-terminal and C-terminal Cas9 fragments fused with dimerization domains were cloned into HindIII/EcoRI and HindIII/XhoI sites of pcDNA3.1 V5/His-A (Invitrogen), respectively. To construct paCas9 nickase and padCas9, we introduced D10A mutation in N-fragment of Cas9 and H840A in C-fragment of Cas9 by multisite-directed mutagenesis kit (MBL) according to manufacturer's directions. The full amino acid sequences of the paCas9-1 and paCas9-2 are shown in **Supplementary Note 1**.

sgRNA constructions. The sgRNAs targeting StopFluc reporters, *CCR5*, *EMX1*, *VEGFA AAVS1* and destabilized luciferase reporter were generated by annealed oligo cloning using BbsI site of Addgene plasmid 47108. The target sequences and oligonucleotides used for sgRNA construction are shown in **Supplementary Table 1**.

Reporter constructions. StopFluc reporters for plasmid HDR assay were constructed by inserting firefly luciferase sequence amplified from pGL4.31 vector (Promega) into HindIII and XhoI sites in pcDNA 3.1/V5-HisA and introducing stop codons and/or mutant PAM by the multisite-directed mutagenesis kit. The site-directed mutagenesis primers used to generate a series of StopFluc reporters are shown in **Supplementary Table 2**. The DNA sequences of StopFluc reporters are also shown in **Supplementary Note 2**. Luciferase donor vector was constructed by inserting inverted firefly luciferase sequence into XhoI and HindIII in bacteria-expression pColdI vector (Clontech). Destabilized luciferase reporter was constructed by inserting firefly luciferase with PEST sequence amplified from pGL4.31 vector into KpnI and XbaI sites in pcDNA 3.1/V5-HisA, and introducing 5 copies of mRNA-destabilizing nonamer sequence[26] (5′-TTATTTATT-3′) into XbaI and ApaI sites by annealed oligo cloning. Surrogate EGFP reporter was constructed by inserting mCherry and out-of frame EGFP into HindIII and XhoI sites in pcDNA 3.1/V5-HisA, and introducing *EMX1* target site between mCherry and EGFP using EcoRI and BamHI sites by annealed oligo cloning.

Cell culture. HEK293T and HeLa cells (ATCC) were cultured at 37 °C under 5% CO_2 in Dulbecco's Modified Eagle Medium (DMEM, Sigma-Aldrich) supplemented with 10% FBS (HyClone), 100 unit/ml penicillin and 100 μg/ml of streptomycin (GIBCO). Cell lines have not been tested routinely for *Mycoplasma* contamination.

Luciferase plasmid HDR assay. HEK293T cells were plated at approximately 2.0×10^4 cells/well in 96-well black-walled plate (Thermo Fisher Scientific), and cultured for 24 h at 37 °C in 5% CO_2. The cells were then transfected with Lipofectamine 2000 (Invitrogen) according to the manufacturer's protocols. Plasmid encoding N-fragments of Cas9 fused with dimerization domain, C-fragments of Cas9 with dimerization domain, sgRNAs, StopFluc reporter and luciferase donor were transfected at a 2.5:2.5:5:1:4 ratio. The total amount of DNA was 0.2 μg/well. Twenty hours after the transfection, samples were incubated at 37 °C in 5% CO_2 under continuous blue light irradiation or in the dark. Blue light irradiation was performed using a 470 nm ± 20 nm LED light source (CCS Inc.). Intensity of blue light was 1.2 W/m^2. For chemically-inducible reassembly of split-Cas9, the culture medium was replaced with 100 μl of DMEM containing 10 nM of rapamycin instead of light irradiation. After 48 h incubation, the culture medium was replaced with 100 μl of phenol red-free DMEM (Sigma-Aldrich) containing 500 μM of D-luciferin (Wako Pure Chemical Industries) as a substrate. After 30 min incubation, bioluminescence measurements were performed using Centro XS^3 LB 960 plate-reading luminometer (Berthold Technologies). For comparison between DNA recognition ability of paCas9 and full-length Cas9, plasmids encoding full-length Cas9, sgRNAs, StopFluc reporter and luciferase donor were transfected at a 5:5:1:4 ratio. The total amount of DNA was 0.2 μg/well. After 48 h incubation, the culture medium was replaced with D-luciferin-containing phenol red-free DMEM and bioluminescence measurements were performed as described above.

Optogenetic genome editing experiments. For NHEJ-mediated indel mutation experiments, HEK293T cells were plated at approximately 1.0×10^5 cells/well in 24-well plate (Thermo Fisher Scientific), and cultured for 24 h at 37 °C in 5% CO_2. The cells were then transfected with Lipofectamine 2000 according to the manufacturer's protocols. Plasmids encoding N713-pMag, nMagHigh1-C714 and sgRNAs were transfected at a 1:1:1 ratio. As a positive control, plasmids encoding full-length Cas9 and sgRNAs were transfected at a 2:1 ratio. The total amount of DNA was 0.9 μg/well. Twenty hours after the transfection, samples were incubated at 37 °C in 5% CO_2 under continuous blue light irradiation or in the dark as described above. After 24 h incubation, genomic DNA was isolated using Blood Cultured Cell Genomic DNA Extraction Mini Kit (Favorgen) according to the manufacturer's instructions.

For HDR-mediated genome editing experiments, 6.0×10^5 HEK293T cells were nucleofected with 125 ng of N713-pMag, 125 ng of nMagHigh1-C714, 250 ng of sgRNA targeting *EMX1* and 10 μM of single-stranded oligonucleotide donor using the SF Cell line 4D-Nucleofector X Kit S (Lonza) and the CA-189 program. Transfected cells were plated at 2.0×10^5 cells/well in 24-well plate. Twenty hours after the nucleofection, samples were incubated at 37 °C in 5% CO_2 under continuous blue light irradiation or in the dark. After 48 h incubation, genomic DNA was isolated as described above.

In **Figure 3f** experiment, cells were plated and cultured as described above NHEJ-mediated indel mutation experiments. The cells were then transfected with Lipofectamine 3000 (Invitrogen) according to the manufacturer's protocols. Plasmids encoding N713-pMag, nMagHigh1-C714 and sgRNAs were transfected at a 1:1:1 ratio. The total amount of DNA was 0.5 μg/well. After 20 h incubation at 37 °C in 5% CO_2 in the dark, samples were incubated at 37 °C in 5% CO_2 under continuous blue light irradiation. After 6 h, we split and incubated the cells in dark and light state. After incubation for 6 h, we performed second transfection of sgRNA targeting *EMX1* with Lipofectamine 3000. The DNA amount was 0.5 μg/well. The samples in dark and light state just before the second transfection were incubated again in dark and light state, respectively. After incubation for 30 h, the genomic DNA was isolated as described above.

Mismatch-sensitive T7E1 assay for quantifying indel mutation of endogenous genes. The genomic region containing paCas9 target site was PCR-amplified using Pyrobest DNA polymerase (TaKaRa) using nested PCR for *CCR5* and *AAVS1* (First PCR: 98 °C, 3 min; (98 °C, 10 s; 55 °C, 30 s; 72 °C, 1 min) × 20 cycles; 72 °C, 3 min. Second PCR: 98 °C, 3 min; (98 °C, 10 s; 55 °C, 30 s; 72 °C, 1 min.) × 35 cycles; 72 °C, 3 min), two-step PCR with 5% DMSO for *EMX1* (98 °C, 3 min; (98 °C, 10 s; 72 °C, 30 s) × 35 cycles; 72 °C, 5 min) or touchdown PCR for *VEGFA* (98 °C, 3 min; (98 °C, 10 s; 72-62 °C, −1 °C/cycle, 30 s; 72 °C, 30 s) × 10 cycles; (98 °C, 10 s; 62 °C, 30 s; 72 °C, 30 s) × 25 cycles; 72 °C, 3 min). The primers for each gene are listed in **Supplementary Table 3**. The PCR amplicons were purified using FastGene Gel/PCR Extraction Kits (Nippon Genetics) following the manufacturer's protocol. Purified PCR products were mixed with 2 μl of 10 × M buffer for restriction enzyme (TaKaRa) and ultrapure water to a final volume of 20 μl, and re-annealed to form heteroduplex DNA (95 °C, 10 min; 90-15 °C, −1 °C/ 1 min). After re-annealing, heteroduplexed DNA were treated with 5 units of T7 endonuclease I (New England BioLabs) for 30 min at 37 °C and then analyzed by agarose gel electrophoresis. Gels were stained with GRR-500 (BIO CRAFT) and imaged with E-shot II gel imaging system (ATTO). Quantification was based on relative band intensities. Following equation is used to calculate the percentage of indel mutation by paCas9: $100 \times (1 - (1 - (b + c)/(a + b + c))^{1/2})$, where a is the intensity of the undigested PCR product, and b and c are the intensities of each T7E1-digested PCR product.

Sequence analysis. Purified PCR products used for the T7E1 assay were inserted into *Eco*RV sites in pcDNA3.1/V5-HisA vector. Plasmid DNAs were isolated by standard alkaline lysis miniprep, and sequenced using a T7 forward primer by the Sanger method.

© 2015 Nature America, Inc. All rights reserved.

RFLP assay for detecting HDR-mediated modification in endogenous human gene. The genomic PCR and purification were performed as described above. Purified PCR products were mixed with 30 units of HindIII (TaKaRa), 2 µl of 10 × M buffer for restriction enzyme and ultrapure water to a final volume of 20 µl, and incubated for 30 min at 37 °C. The digested products were analyzed by agarose gel electrophoresis. Gel staining and imaging were performed as described above. Quantification was based on relative band intensities. Following equation is used to calculate the percentage of HDR by paCas9: 100 × (b + c)/(a + b + c), where a is the intensity of the undigested PCR product, and b and c are the intensities of each HindIII-digested product.

Spatial surrogate reporter activation. HEK293T cells were plated at 8.0×10^5 cells/dish on 35 mm dish (Iwaki Glass) coated with fibronectin (BD Biosciences), and cultured for 24 h at 37 °C in 5% CO_2. The cells were then transfected with Lipofectamine 2000 according to the manufacturer's protocols. Plasmids encoding N713-pMag, nMag-Cas9, sgRNAs targeting *EMX1* and NHEJ-mediated surrogate EGFP reporter containing *EMX1* targeting site were transfected at a 1:1:2:6 ratio. The total amount of DNA was 4.0 µg/dish. Twenty hours after the transfection, samples were illuminated by slit-patterned blue light using a photomask for 24 h at 37 °C in 5% CO_2. The width of slit is 2 mm. Cells were fixed with 4% paraformaldehyde in PBS for 15 min. Images were acquired using Axio Zoom.V16 stereo zoom microscope (Zeiss), and analyzed using Metamorph (Molecular Devices).

Photoactivatable CRISPR interference. HEK293T cells were plated at 2.0×10^4 cells/well in 96-well black-walled plate, and cultured for 24 h at 37 °C in 5% CO_2. The cells were then transfected with Lipofectamine 3000 according to the manufacturer's protocols. Plasmids encoding N713 (D10A)-pMag, nMag-Cas9 (H840A), mRNA-destabilized luciferase-PEST reporter and indicated sgRNAs targeting luciferase reporter were transfected at a 2.5:2.5:1:4 ratio. As a full-length dCas9 control, plasmids encoding full-length dCas9, mRNA-destabilized luciferase-PEST reporter and indicated sgRNAs were transfected at a 5:1:4 ratio. For the sample transfected with triple sgRNAs, the ratio of three sgRNAs was 1:1:1. The total amount of DNA was 0.1 µg/well. In **Figure 4b**,**c** experiments, 20 h after the transfection, samples were incubated at 37 °C in 5% CO_2 under continuous blue light irradiation or in the dark as described above. After 30 h, the culture medium was replaced with 100 µl of phenol red-free DMEM containing 500 µM of D-luciferin. After 1 h incubation, bioluminescence measurements were performed. In **Figure 4d** experiment, samples were incubated at 37 °C in 5% CO_2 under continuous blue light immediately after transfection. After 30 h, the culture medium was replaced with phenol red-free DMEM containing D-luciferin as described above. After 1 h incubation, light-illuminated samples were incubated again upon continuous blue light or in the dark, and bioluminescence measurements were performed at indicated time points.

Reproducibility and statistics. No sample size estimates were performed, and our sample sizes are consistent with that normally used in the genome editing and gene regulation experiments. No sample exclusion was carried out. No randomization was used. No blinding was used. In **Figures 3b** and **4b**,**c**, variances estimated by *F*-tests were equal, and two-sided Welch's *t*-tests were performed. We also confirmed the same statistical results by nonparametric two-sided Mann-Whitney tests because the normality of data was not tested. *P* values by Mann-Whitney tests are following; In **Figure 3b**, paCas9-1 and paCas9-2 in light showed no significant difference: $P = 0.773$. In **Figure 4b**, light and dark samples transfected with padCas9 targeting luciferase showed significant differences: $P = 0.00395$. Light and dark samples transfected with padCas9 and negative control sgRNA showed no significant difference: $P = 0.749$. In **Figure 4c**, padCas9 and full-length dCas9 transfected with sgFluc-1, sgFluc-2 and sgFluc-1+2+3 showed significant differences: $P = 0.00395$ (sgFluc-1), $P = 0.0065$ (sgFluc-2), $P = 0.00395$ (sgFluc-1+2+3), respectively. padCas9 and full-length dCas9 transfected with sgFluc-3 showed no significant difference: $P = 0.109$.

© 2015 Nature America, Inc. All rights reserved.

doi:10.1038/nbt.3245